JACS
JOURNAL OF THE AMERICAN CHEMICAL SOCIETY
Communication
pubs.acs.org/JACS

Enhancing Raman Scattering without Plasmons: Unprecedented Sensitivity Achieved by TiO_2 Shell-Based Resonators

Ivano Alessandri*

INSTM and Chemistry for Technologies Laboratory, University of Brescia, via Branze 38, 25123 Brescia, Italy

Supporting Information

ABSTRACT: A remarkable enhancement of Raman scattering is achieved by TiO_2 shell-based spherical resonators in the absence of plasmonic enhancers. This effect is ascribed to the synergistic combination of high refractive index of the shell layer, multiple light scattering through the spheres, and related geometrical factors and can be exploited to fabricate a new generation of self-diagnostic, recyclable SERS-active substrates.

Surface-enhanced Raman scattering (SERS)[1] is a leading nondestructive technique that can extend the sensitivity of Raman spectroscopy to the level of a single molecule.[2] It relies on the exploitation of surface plasmon−polariton near-field generated by interaction of a light source with an active substrate, which is generally made of coinage metals (Au, Ag, Cu, as their surface plasmon resonance is in the visible or near-infrared region of the electromagnetic radiation) in the form of either nanoparticles, nanostructures, or electrochemically roughened surfaces.[3] However, for a number of important applications, such as *in situ* Raman monitoring of chemical reactions,[4] plasmon-based SERS substrates can introduce strong perturbations into the systems under investigation and promote photothermal and/or photochemical reactions.[5] This prevents extraction of unbiased data and represents a still unsolved major drawback. Metal-free SERS has been demonstrated using quantum dots[6] or semiconductor nanostructures[7] and nanoparticles (including TiO_2).[8] In all of these cases, charge transfer at the semiconductor−analyte interface plays a major role in Raman scattering enhancement. An alternative approach to investigate the Raman vibrational features of surface layers is attenuated total reflection (ATR-Raman), where the analyte is probed by the evanescent field emerging from high-refractive-index prisms.[9,10] However, ATR-Raman and, in general, total reflection Raman scattering (TRRS) techniques are not so extensively employed as the analogous infrared counterparts, because their sensitivity is low and experimental equipment is quite impractical. Total internal reflection within dielectric microspheres (microresonators) gives rise to evanescent electromagnetic fields that can generate local surface "hot spots" (whispering-gallery-mode (WGM) resonances), which are commonly used in optical sensing.[11] In a theoretical paper, Ausman and Schatz predicted that when the Raman scattered radiation overlaps with a WGM resonance, enhancement factors comparable to those usually observed with noble metals can be reached.[12] However, in spite of its potential, cavity-enhanced Raman scattering (CERS) has been so far underdeveloped, with only few examples limited to alcohol/water microdroplets or silica microspheres that take advantage of silver coatings to enhance Raman intensity.[13]

Here we demonstrate for the first time that a remarkable enhancement of Raman sensitivity can be obtained in the absence of plasmonic nanostructures by means of TiO_2 shell-based spherical resonators. The synergistic combination of high refractive index of the shell layer, multiple light scattering through the spheres, and related geometrical factors allowed both self-diagnostic Raman analysis of thin and ultrathin (5 nm or less) layers of anatase-TiO_2 and direct monitoring of photocatalytic reactions under operando-like conditions. Moreover, thanks to the self-cleaning properties of anatase under UV irradiation, these substrates are recyclable: different analytes and reactions can be monitored and directly compared using the same active surface.

The TiO_2 resonators (T-rex) used in this paper consist of monodisperse core/shell SiO_2/TiO_2 microspheres. The SiO_2 cores were assembled in the form of mono- or multilayers onto planar substrates (single-crystal Si or glass slides) and coated by different conformal shell layers of amorphous TiO_2, with thicknesses of 5, 10, 20, 50, and 100 nm, by atomic layer deposition (ALD). Subsequent annealing yielded fully crystalline anatase (see experimental details in the Supporting Information (SI) and Figure 1).

Figure 2a shows the micro-Raman spectra of spherical resonators achieved by depositing a 100-nm-thick TiO_2 film onto microsphere assemblies (T-rex100 samples). Raman spectra were acquired from both mono- and multilayered regions and compared to planar films grown on the same substrate during the ALD process. This experimental design ensures the comparability between titania layers achieved by the same number of ALD cycles and annealed exactly under the same conditions. The Raman spectra of anatase grown on T-rex spheres show a remarkable enhancement in their intensity in comparison to the planar reference. Using the same acquisition parameters, all of the typical anatase Raman-active modes ($E_{g(1)}$, $E_{g(2)}$, $A_{1g}+B_{1g(2)}$, and $E_{g(3)}$) can be observed for T-rex in both mono- and multilayered configuration. In spite of the short acquisition time, the signals are very intense and characterized by an excellent signal-to-noise ratio. On the other hand, the planar film can hardly be detected (see magnification in the inset of Figure 2a), and the whole information is restricted to the main anatase peak ($E_{g(1)}$ mode), whereas $E_{g(2)}$ is undetectable. The remaining anatase modes

Received: February 15, 2013
Published: April 5, 2013

 © 2013 American Chemical Society dx.doi.org/10.1021/ja401666p | J. Am. Chem. Soc. 2013, 135, 5541−5544

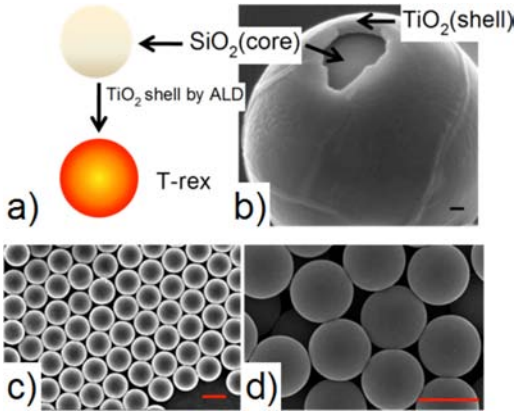

Figure 1. (a) Scheme of preparation of TiO_2 spherical resonators (T-rex). The silica cores are conformally coated with an amorphous titania thin shell by atomic layer deposition (ALD). Annealing at 700 °C (6 h) promotes the formation of crystalline anatase. (b) SEM image showing a T-rex100 sample. Surface fracture allows us to see the SiO_2 core and evaluate the thickness of the titania layer. Scale bar: 100 nm. (c) Low- and (d) high-magnification SEM images of T-rex20 samples. Scale bars: 2 μm.

closely approach the detection limit and are characterized by a very poor signal-to-noise ratio.

This effect becomes even more dramatic when lower TiO_2 thicknesses are considered. Planar substrates do not allow titania film with thicknesses below 50 nm to be detected with a signal-to-noise ratio sufficient for any analytical purposes. In contrast, T-rex spheres can extend the detection limit down to few unit cells. Figure 2b shows the spectrum of a 5-nm-thick layer of anatase grown onto spherical cores (T-rex5). No Raman signals can be observed from the same anatase film deposited onto planar substrates, and results are negative even with a very long (10 min) acquisition time. These results indicate that the self-diagnostic capability of T-rex can reach very high sensitivity levels, with interesting extensions to the ultrathin film domain.

The statistical analysis of the intensity ratios of the anatase main peak ($E_{g(1)}$ mode, around 143 cm^{-1}) of T-rex 100, normalized to the corresponding planar reference (Figure 3a), confirms this trend, revealing that the Raman intensity of the planar film is less than 2.5% of that exhibited by T-rex monolayers and less than 1% of that achievable from multilayered regions (≥5 layers). Raman scattering data are quite reproducible and show that the spectra obtained from multilayers are significantly more intense than those coming from a monolayer, although the number of ALD cycles (i.e., the amount of titania deposited onto the cores) is the same. No significant differences in Raman scattering intensity were found comparing monolayered and isolated T-rex spheres. This can be explained by the lateral resolution of the laser beamsize used in the present experimental setup, which is below 2 μm, allowing single T-rex spheres to be sorted from a close-packed monolayer.

A detailed evaluation of Raman scattering as a function of the number of T-rex layers revealed that the Si peak originated from the underlying substrate disappears when the number of stacked T-rex spheres is >3. (Figure 3b) This means that the exciting laser is completely entrapped within T-rex colloidal crystals. Thus, the whole contribution to the Raman scattering originates from only T-rex spheres and is not dissipated by interactions with the substrate. On the basis of these findings

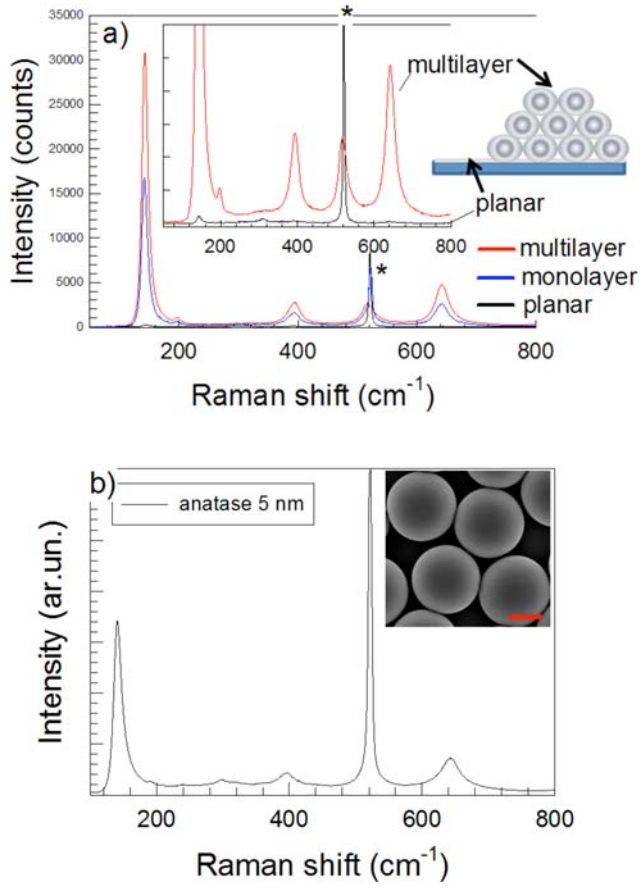

Figure 2. (a) Comparison between Raman spectra of a 100-nm-thick anatase layer deposited on either a planar substrate or silica microspheres (mono- or multilayered, T-rex100 samples). The peak of the Si substrate at 520 cm^{-1}, observed only for planar and monolayered samples, is indicated by an asterisk. The spectra were acquired with a He−Ne laser (λ = 633 nm) focused through a 100× objective (N.A. 0.9) for 5 s. (b) Raman spectrum of a 5-nm-thick anatase layer deposited on silica microspheres (T-rex5). The spectrum was acquired for 60 s under the above-described conditions. The SEM image of this sample is shown in the inset. Scale bar: 1 μm.

we may hypothesize that the remarkable enhancement exhibited by T-rex spheres is due to the synergistic contribution of two main factors:

(1) TiO_2 is a high-refractive-index shell ($n \approx 2.5$ for the anatase) between two lower refractive index media (air, $n = 1$ and SiO_2, $n \approx 1.45$). The refractive index contrast can allow for total internal reflection of light within the titania shell layer.

(2) When the T-rex spheres are assembled as colloidal crystals, they play as extended Fabry−Pérot cavities, giving rise to multiple light scattering. Examples of these phenomena can be observed in the optical reflectance spectra shown in Figure S2.

These factors concur to strongly increment the optical path of the photons within the spheres and the consequent stimulation of Raman scattering. The contribution of the internal reflection is further corroborated by a couple of experimental observations. First, analogous experiments carried out using resonators made of TiO_2 hollow shells (T-horex) show a slight (1.2) yet statistically relevant enhancement of the Raman signal in comparison to that observed for T-rex samples

dx.doi.org/10.1021/ja401666p | J. Am. Chem. Soc. 2013, 135, 5541−5544

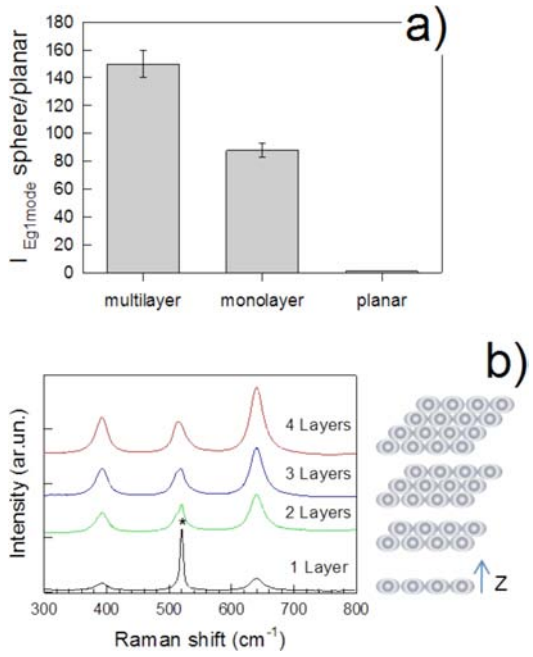

Figure 3. (a) Evaluation of the anatase $E_{g(1)}$ mode intensity ratio between T-rex100 samples and the corresponding planar reference. Data reported in this histogram resulted from Raman spectra acquired over 30 different regions per sample and provide an indication of the enhancement factor for this Raman mode. (b) Raman spectra as a function of the number of T-rex layers. The Si substrate peak, indicated by an asterisk, was taken as a reference to evaluate the minimum number of T-rex layers required for light trapping.

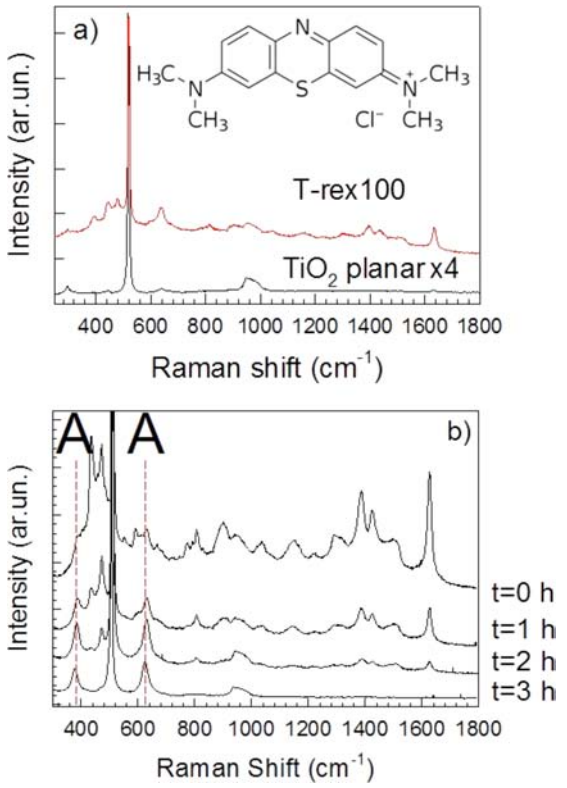

Figure 4. a) Raman spectrum of a 10^{-5} M MB solution adsorbed on a T-rex 100 sphere. The spectrum of the same solution adsorbed on a 100 nm-thick anatase planar film (multiplied by 4) is shown for a comparison; b) monitoring of UV-induced photodegradation of MB adsorbed on a T-rex 100 sphere as a function of irradiation time. The initial concentration (t = 0) of the MB solution was 10^{-4} M. The $B_{1g(1)}$ and $E_{g(3)}$ anatase modes are indicated by a dashed line.

with the same size (see SI 3a) The hollow shell configuration increases the refractive index contrast (n TiO_2 shell/n core) because the inner core is made of air (n = 1) instead of SiO_2 (n = 1.45). Second, when the shell is made of materials with a lower refractive index such as ZnO (n = 1.98) (and, as a consequence, the spherical resonators have lower shell/core refractive index contrast) no significant Raman enhancements are observed in comparison with the planar reference, neither for mono- nor for multilayers, although multiple Fabry-Pérot reflections are almost the same to those observed for T-rex, because they only depend on sphere size, packing (including defects) and thickness of the colloidal crystal. A more detailed discussion on the origin of the enhanced Raman scattering, including additional factors such as the size of spherical resonators, microsphere-induced overfocusing of the exciting Gaussian laser beam and consequent strong surface confinement of the electromagnetic field, is reported in SI 3b,c.

The evanescent electromagnetic field originated by the optical effects described above is expected to assist the detection of analytes adsorbed at the T-rex surface and, as a consequence, the investigation of related interfacial processes. As a proof-of-concept experiment we tested the detection of Methylene Blue (MB) adsorbed at the T-rex surface and its degradation under UV light irradiation. The photodegradation reaction was monitored by selecting specific spheres by direct optical microscope inspection. Figure 4a shows the Raman spectra of a T-rex100 monolayered sample which has been incubated with a 10^{-5} M solution of MB. Although this concentration is below the detection limit of MB adsorbed on titania planar thin film substrates, T-rex supports show MB spectra characterized by intense modes and excellent signal-to-noise ratio. This increased sensitivity can be related to the evanescent field generated at the TiO_2/MB interface. Although still far from the detection throughput achievable with conventional metal-based SERS substrates, T-rex allows to extend the Raman sensitivity to a concentration range which is suitable for monitoring many reactions of practical interest (degradation of organic pollutants, water-splitting, etc.). Most important, these processes can be investigated without the interference of any metallic enhancers. In the present case we can observe that the MB signals undergo a progressive decrease as a function of irradiation time and eventually disappear in the spectrum acquired after 3 h (Figure 4b).

Before irradiation a significant amount of MB is adsorbed at the TiO_2 interface in form of dimers or molecular aggregates, as indicated by the strong C−N−C bending mode at 450 cm^{-1}. After 1 h this mode is strongly reduced in comparison to the 481 cm^{-1} thiazine ring in-plan bending mode, which characteristic of monomeric MB.[14] As MB is removed from the surface the anatase modes become more evident. Interestingly, the anatase signals are slightly stronger in the spectrum acquired after 2 h, when some MB is still adsorbed on the TiO_2 surface, than after 3 h, i.e., when MB has been completely removed (the Si peak was taken as an internal reference). This result agrees with the observations reported by Lombardi and co-workers about the enhancement of titania phonon modes induced by coupling with organic dyes.[15] This phenomenon and its dependence on wavelength and dye concentration is still under investigation.

dx.doi.org/10.1021/ja401666p | J. Am. Chem. Soc. 2013, 135, 5541−5544

Once MB has been fully decomposed, T-rex supports can be thoroughly washed (water and ozone-UV cleaner) to remove any degradation byproducts and reused for testing other reactions (identical or different) occurring exactly at the same place. Recyclability exploits the photocatalytic activity of anatase and is described in more detail in SI 5.[16] In conclusion, we have demonstrated that TiO_2-based spherical resonators (T-rex) are powerful tools for non-plasmon-assisted surface enhanced Raman spectroscopy. They outperform the detection limits of planar substrates, extending the self-diagnostic capability of TiO_2 interfaces to the level of few lattice cells. The extraordinary scattering of the exciting light allows analytes and their interactions with the TiO_2 surface to be investigated under operando-like conditions. Direct optical tracking and recyclability offer exciting possibilities in view of comparing different processes occurring at the same interface.

In perspective, different high-refractive index materials and architectures can be tested and integrated into optical-fiber based devices. This general approach could be also extended to infrared and fluorescence spectroscopy, in order to fabricate multiplex sensors for the simultaneous acquisition of different spectroscopic information.

■ ASSOCIATED CONTENT

Supporting Information

Experimental details, including UV−vis characterization, recyclability Raman experiments, and discussion on the enhancement mechanism. This material is available free of charge via the Internet at http://pubs.acs.org.

■ AUTHOR INFORMATION

Corresponding Author

ivano.alessandri@ing.unibs.it

Notes

The authors declare no competing financial interest.

■ ACKNOWLEDGMENTS

Dr. Marco Salmistraro and Dr. Matteo Ferroni are acknowledged for assistance in ALD deposition and SEM analysis, respectively. Prof. Luigi Sangaletti and John R. Lombardi are acknowledged for stimulating discussions. Emma Alessandri is acknowledged for inspiring "resonating" insights. This work was supported by a “PID” grant-in-aid project from the Mechanical and Industrial Engineering Department of the University of Brescia.

■ REFERENCES

(1) (a) Jeanmarie, D. L.; Van Duyne, R. P. *J. Electroanal. Chem.* **1977**, *84*, 1. (b) Albrecht, M. G.; Creighton, J. A. *J. Am. Chem. Soc.* **1977**, *99*, 5215.

(2) (a) Nie, S.; Emory, S. R. *Science* **1997**, *275*, 1102. (b) Kneipp, K.; Wang, Y.; Perelman, L. T.; Itzkan, I.; Dasari, R. R.; Feld, M. S. *Phys. Rev. Lett.* **1997**, *78*, 1667.

(3) (a) Aroca, R. *Surface-Enhanced Vibrational Spectroscopy*; John Wiley & Sons: New York, 2006. (b) Le Ru, E. C.; Etchegoin, P. G. *Principles of Surface-Enhanced Raman Spectroscopy*;Elsevier: Amsterdam, 2009. (c) Lombardi, J. R.; Birke, R. L. *Acc. Chem. Res.* **2009**, *42*, 734.

(4) Weckhuysen, B. M. *Angew. Chem., Int. Ed.* **2009**, *48*, 4910.

(5) Alessandri, I.; Ferroni, M. *J. Mater. Chem.* **2009**, *19*, 7990.

(6) Quagliano, L. G. *J. Am. Chem. Soc.* **2004**, *126*, 7393.

(7) Wang, X. T.; Shi, W. S.; She, G. W.; Mu, L. X. *J. Am. Chem. Soc.* **2011**, *133*, 1658.

(8) Musumeci, A.; Gosztola, D.; Schiller, T.; Dimitrijevic, N . M.; Mujica, V.; Martin, D.; Rajh, T. *J. Am. Chem. Soc.* **2009**, *131*, 6040.

(9) Ikeshoji, T.; Ono, Y.; Mizuno, T. *Appl. Opt.* **1973**, *12*, 2236.

(10) Woods, D. A.; Bain, C. D. *Analyst* **2012**, *137*, 35.

(11) Arnold, S.; Keng, D.; Shopova, S. I.; Holler, S.; Zurawsky, W.; Vollmer, F. *Opt. Express* **2009**, *17*, 6230.

(12) Ausman, L. K.; Schatz, G. C. *J. Chem. Phys.* **2008**, *129*, 054704.

(13) (a) White, I. M.; Gohring, J.; Fan, X. *Opt. Express* **2007**, *15*, 17433. (b) White, I. M.; Hanumegowda, N. M.; Oveys, H.; Fan, X. *Opt. Express* **2005**, *13*, 10754.

(14) Alessandri, I.. *J. Colloid Interface Sci.* **2011**, *351*, 576.

(15) Ma, S.; Livingstone, R.; Zhao, B.; Lombardi, J. R. *J. Phys. Chem. Lett.* **2011**, *2*, 671.

(16) Vukicevic, U.; Ziemian, S.; Bismarck, A.; Shaffer, M. S. P. *J. Mater. Chem.* **2011**, *18*, 3448.